Broad-Band Dielectric Spectroscopy on the Molecular Dynamics of Bulk and Adsorbed Poly(dimethylsiloxane)

K. Ulrich Kirst,*,† Friedrich Kremer,† and Victor M. Litvinov‡

Max-Planck-Institut für Polymerforschung, Postfach 3148, W-6500 Mainz, FRG, and Institute of Synthetic Polymer Materials, Academy of Sciences of Russia, Profsoysnaya ul.70, 117393 Moscow, Russia

Received February 6, 1992; Revised Manuscript Received October 26, 1992

ABSTRACT: Broad-band dielectric spectroscopy (10^{-1}–10^{6} Hz) was employed to compare the molecular dynamics of poly(dimethylsiloxane) (PDMS) and its mixtures with hydrophilic and hydrophobic Aerosil (fumed silica). After quenching from ambient temperature and subsequent reheating to about 150 K, pure PDMS exhibits the α-relaxation in the amorphous state. At higher temperatures the α_c-relaxation process, which is assigned to the relaxation of the amorphous fraction in the semicrystalline polymer, is observed. Filled PDMS shows in contrast three distinct relaxation processes which originate from the varying degree of interaction with the filler surface. These processes are assigned to the relaxation of directly bound, interfacial, and nonadsorbed PDMS in the mixture. Restrictions of chain motions in the adsorption layer are smaller for the mixture with hydrophobic Aerosil in comparison with the hydrophilic one. The results are compared with previous NMR data for the same systems.

1. Introduction

The molecular dynamics of pure PDMS has been studied by a variety of spectroscopic techniques such as NMR,[1] light scattering,[2] ESR,[3] mechanical, and dielectric spectroscopy.[4–6] Early studies of adsorption kinetics,[7] the viscosity of the boundary layer,[8] and molecular mobility[7,9] in PDMS–adsorbent systems revealed that molecular motions of chain units adjacent to an adsorbent surface are different from those in the bulk. In the present paper dielectric spectroscopy is employed to study molecular dynamics of mixtures of PDMS with hydrophilic and hydrophobic Aerosil in a broad frequency range.

2. Experimental Section

2.1. Preparation of Filled PDMS. Linear PDMS ($(CH_3)_3SiO[Si(CH_3)_2]_nSi(CH_3)_3$, $n \approx 70$) with trimethylsilyl end groups was prepared by anionic nonequilibrium polymerization of hexamethylcyclotrisiloxane.[10] Molecular weight M_W and molecular weight distribution (M_W/M_N) are 5300 and 1.03, respectively. Two types of Aerosil were used for the preparation of mixtures. One (Aerosil A 380) contains hydrophilic surface OH groups which are the sites of adsorption. The surface of another one, Aerosil R 812, bears hydrophobic trimethylsilyl groups. Aerosils A 380 and R 812 supplied by Degussa have a specific particle surface of 380 ± 30 and 260 ± 30 m^2/g, respectively, and an average particle diameter of 7 nm (trade grade). The volume fraction of Aerosil in the mixtures was 50 vol % for the densities of PDMS and Aerosil of 0.982 and 2.20 g/cm^3, respectively.

The preparation of PDMS–Aerosil mixtures included the following steps: (1) Aerosil was evacuated in a retort under vacuum of 1.3 mbar at 500 K for 10 h. (2) The retort was filled by argon for protection from humidity. (3) A 0.5 weight % solution of PDMS in *n*-pentane was added. (4) The solution was stirred for 2 days, and the solvent was removed under vacuum at 400 K for 4 h. (5) The resulting powder samples were pressed to pellets at pressures of about 30 MPa. The pellets were transfered to the sample capacitors. Handling in air took about 3–5 min. Preparation of pure Aerosils for measurements consisted only of the first and the second step.

Before the dielectric measurements all samples were quenched in liquid nitrogen starting from ambient temperature at a cooling rate higher than 60 K/min to prevent crystallization. In the studied mixtures the degree of crystallinity is negligible even without quenching.[9,11] The samples were placed in custom-made cryostats wherein their temperature was regulated by a stream of temperature-controlled nitrogen gas. This method allows temperature adjustment from 100 up to 500 K with a stability of ±0.02 K.[12] During the dielectric measurements the samples were reheated stepwise. Each temperature was held for 1 h.

2.2. Dielectric Measurement Systems. The dielectric experiments in the frequency range 10^{-1} to 10^{6} Hz were carried out by measuring the complex impedance of a sample-filled capacitor with a Solartron-Schlumberger frequency response analyzer FRA 1260 supplemented by a high-impedance preamplifier of variable gain.[13] The relative accuracy of the measurement systems for samples having a dielectric loss of 10^{-2} is ±1% in ϵ' and ±3% in ϵ''. The sample capacitor consisted of two gold-plated brass plates (diameter 40 and 20 mm, respectively) and was filled with a pellet of the mixture, the average thickness of which ranged between 40 and 220 μm with an accuracy ±2 μm. The degree of filling of the sample capacitor was determined by weighing. The uncertainty in the determination of the absolute value of the filling factor is estimated to be ±20% and hence the absolute value of the dielectric relaxation strength has a similar error. For the experiments with the pure filler, the powder was pressed between the capacitor plates. In a similar way the preparation of the capacitors with pure unfilled PDMS was carried out. A sample thickness of 50 ± 1 μm was maintained by use of glass-fiber spacers.

To describe the dielectric spectra quantitatively the relaxation function of Havriliak–Negami[14,15] was used:

$$\epsilon = \epsilon_\infty + \frac{\epsilon_{st} - \epsilon_\infty}{(1 + (i\omega\tau)^\alpha)^\beta} \tag{2.1}$$

In this notation ϵ_∞ stands for the real part of the dielectric function at $\omega\tau \gg 1$ and ϵ_{st} the corresponding value for $\omega\tau \ll 1$. The dielectric relaxation strength $\Delta\epsilon$ is defined by $\Delta\epsilon = \epsilon_{st} - \epsilon_\infty$. α characterizes the logarithmic slope of the low-frequency wing of the function and the product $\alpha\beta$ the one on the high-frequency side. This means that broad relaxation time distributions are characterized by small values for α and β. τ is the mean relaxation time. The frequency at maximum loss is denoted by f_{max}.

A conductivity contribution was observed at frequencies below 10^4 Hz. It can be described by the power law

$$\epsilon'' = \frac{\sigma_0}{\epsilon_0}\omega^{s-1} \tag{2.2}$$

where σ_0 and s are fitting parameters.[16] σ_0 is a constant of proportionality and ϵ_0 denotes the permittivity of free space. The dielectric data were fitted to combinations of one or two Havriliak–Negami functions and a conductivity contribution. From the fitted parameters, i.e. τ, $\Delta\epsilon$, α, and β, the mean relaxation

† Max-Planck-Institut für Polymerforschung.
‡ Institute of Synthetic Polymer Materials.

0024-9297/93/2226-0975$04.00/0

times as well as the maximum frequencies and the widths of the single relaxation processes were calculated. In fits of spectra at different temperatures, the shape-parameters α and β of the Havriliak–Negami function for the three processes were varied only slightly. This procedure reduces the uncertainty of the fitted parameters, which is ±10% in $\Delta\epsilon$, ±0.03 in α and β, and between 0.07 and 0.65 (for very broad relaxations) decades in τ. Alternatively, the temperatures corresponding to given peak frequencies could be determined from ϵ'' vs T plots with an uncertainity of ±1 K for narrow and ±5 K for broad relaxations.

The temperature dependence of relaxation processes, which are related to the glass transition, can be well described by the Williams–Landel–Ferry (WLF) equation[17] within the region $T_g < T < T_g + 100$ K.[18] With $f = 1/2\pi\tau$ this is written as

$$\log \frac{f(T)}{f(T_0)} = \frac{C_1(T - T_0)}{C_2 + T - T_0} \tag{2.3}$$

where T_0 is a reference temperature, which is defined in this paper by the relation $f(T_0) = 1$ Hz. According to[17,19,20] the fitted parameters C_1 and C_2 are connected to the fractional free volume v_f/v at glass transition temperature and its thermal expansion coefficient α_f: $v_f/v(T_g) = (2.303C_1)^{-1}$ and $\alpha_f = (2.303C_1C_2)^{-1}$

For comparison between dielectric and NMR data it must be taken into consideration that, in general, the dielectric relaxation time τ_{Diel} is not the same as the nuclear resonance correlation time τ_{NMR}.[21] The relation $3\tau_{NMR} = \tau_{Diel}$ holds for the model of spheres moving in a viscous medium.[22] Thus, frequencies of molecular motions previously obtained by NMR were divided by a factor of 3.

From the Fröhlich equation for the dielectric strength $\Delta\epsilon$ the following expression can be extracted:

$$\Delta\epsilon = \gamma n \mu^2 \tag{2.4}$$

where μ denotes the electric dipole moment of the chain units, n the number density, and γ the Kirkwood–Fröhlich correlation factor,[23] which is inversly proportional to temperature. Hence a measurement of $\Delta\epsilon$ allows an estimate of the fraction of the dipoles involved in the different relaxation processes. In representation vs temperature, ϵ'' can be discribed by combinations of the Havriliak–Negami function (eq 2.1) and the WLF equation (eq 2.3) with eq 2.4, i.e. $\Delta\epsilon = \Delta\epsilon_0 T_0/T$ and $\tau = \tau_0 \exp[-C_1(T - T_0)/(C_2 + T - T_0)]$. The result is

$$\epsilon = \epsilon_\infty + \frac{\Delta\epsilon_0 T_0/T}{\left(1 + \left(i\omega\tau_0 \exp\left(\frac{-C_1(T - T_0)}{C_2 + T - T_0}\right)\right)^\alpha\right)^\beta} \tag{2.5}$$

3. Results and Discussion

An analysis of the data for filled systems requires the detailed knowledge of the dielectric data of the pure systems. Therefore, in the first two sections, the measurements on pure PDMS and on pure Aerosils are presented.

3.1. Pure PDMS. PDMS forms a crystalline phase in the temperature range below (230 K).[25] In order to avoid crystallization PDMS was quenched from room temperature in liquid nitrogen down to 78 K. Such thermal treatment allows obtaining PDMS in an amorphous supercooled state.[24,25] In the temperature range between 147 and 156 K (Figure 1) the α-relaxation peak[4] is observed, it has a half-width of 2.3 decades and a strength $\Delta\epsilon$ of 0.71. This peak is assigned to the relaxation of amorphous PDMS.[26] A few degrees above T_g, at 156 K, its relaxation strength $\Delta\epsilon$ decreases strongly while at lower frequencies a second relaxation grows in strength (Figure 1) with a half-width of about 4.5–5.3 decades. It supersedes the α-relaxation completely at temperatures above 158 K. Its strength $\Delta\epsilon$ approaches 0.22. Since cold crystallization takes place in amorphous PDMS above T_g,[24] the strong change of dielectric losses with increasing temperature can obviously be explained by a replacement of the

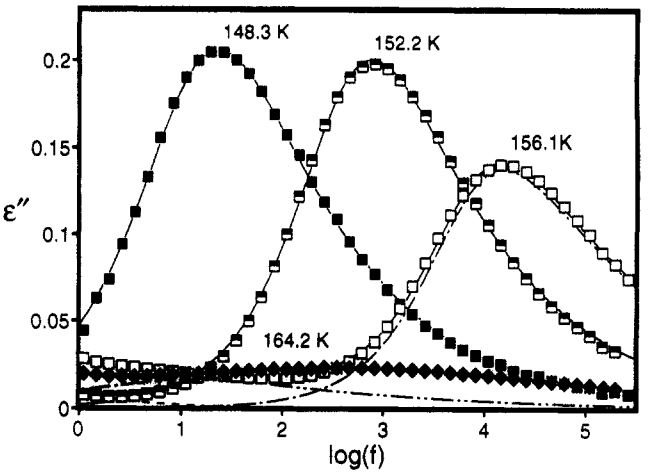

Figure 1. Dielectric loss ϵ'' vs frequency for pure PDMS at different temperatures in the amorphous phase (■, ⊟, and □) and after cold crystallization (♦). The solid lines describe the fits using eqs 2.1 and 2.2. The error in ϵ'' is not larger than the size of the symbols.

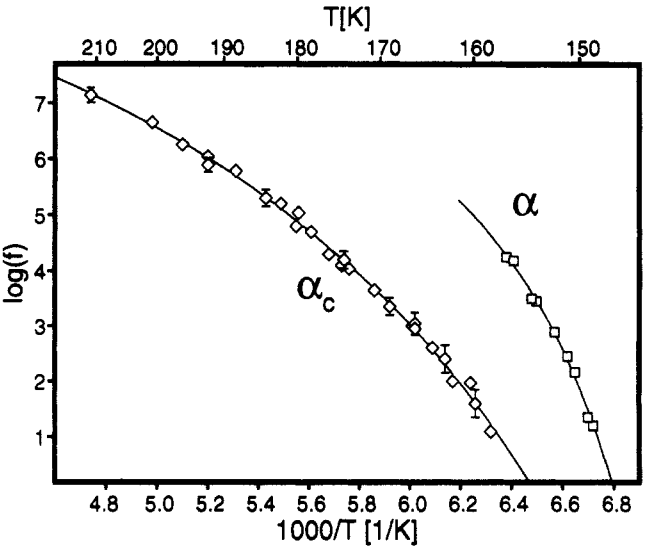

Figure 2. Havriliak–Negami relaxation frequency f vs inverse temperature of the α-relaxation of pure amorphous PDMS and of the α_c-relaxation of the semicrystalline sample. The lines show WLF plots of the processes (see Table II) corresponding to eq 2.3.

α-process by the slower and broader α_c-relaxation. The latter is assigned to motions of constrained partial chains between crystalline lamellae, i.e. of units in chain bows and loops between the points where the chains enter crystals.[26] The $\Delta\epsilon$ of the α_c-relaxation is small in comparison with the α-relaxation because the relaxation of dipoles within the crystalline phase is strongly suppressed. From the decrease in $\Delta\epsilon$ a degree of crystallinity of about 72% can be estimated according to eq 2.4. The α_c-relaxation showed a broad relaxation time distribution. Parameters from Havriliak–Negami fits and WLF parameters corresponding to fits given in Figures 1 and 2 are listed in Table I and in Table II, respectively. It turned out that transition temperature and speed of the cold crystallization are very sensitive to thermal history.

3.2. Pure Fillers. Dielectric data for pure Aerosil are shown in Figure 3a. One relaxation process is observed for hydrophobic and hydrophilic Aerosil. The maximum of the relaxation peak for hydrophobic Aerosil is near 0.012, while the activation energy (Figure 3b) amounts to about 44 ± 5 kJ/mol. In the case of hydrophilic Aerosil about 4 times stronger relaxation peaks at higher frequencies,

Table I
Havriliak–Negami Fit Parameters with Error Estimations for Some Dielectric Spectra

	temp/K	$\Delta\epsilon$	α	β	$-\log(\tau/s)$
pure quenched PDMS					
first relaxation	148.3	0.71 ± 0.15	0.82 ± 0.02	0.49 ± 0.03	1.8 ± 0.05
	150.3	0.68 ± 0.14	0.86 ± 0.02	0.46 ± 0.03	2.60 ± 0.05
	153.8	0.60 ± 0.12	0.86 ± 0.03	0.45 ± 0.03	3.9 ± 0.05
	156.1	0.56 ± 0.11	0.84 ± 0.05	0.40 ± 0.05	4.6 ± 0.08
second relaxation	158.1	0.20 ± 0.04	0.28 ± 0.03	0.65 ± 0.03	1.21 ± 0.25
	160.1	0.20 ± 0.04	0.31 ± 0.03	0.63 ± 0.03	1.85 ● 0.20
	168.2	0.22 ± 0.04	0.35 ± 0.03	0.55 ± 0.03	2.96 ± 0.18
	176.3	0.17 ± 0.03	0.37 ± 0.03	0.50 ± 0.03	4.15 ± 0.15
	184.6	0.17 ± 0.03	0.35 ± 0.03	0.50 ± 0.03	4.68 ● 0.13
	192.4	0.14 ± 0.03	0.36 ± 0.03	0.49 ± 0.03	5.82 ● 0.13
hydrophilic Aerosil	148.9	0.31 ± 0.06	0.31 ± 0.04	0.99 ± 0.01	3.70 ● 0.15
	153.7	0.31 ± 0.06	0.33 ± 0.03	1.00 ± 0.01	3.18 ± 0.15
	158.3	0.31 ± 0.06	0.36 ± 0.03	0.84 ± 0.02	4.36 ± 0.15
	163.1	0.30 ± 0.06	0.38 ± 0.02	1.00 ± 0.02	4.96 ± 0.15
	176.5	0.25 ± 0.05	0.38 ± 0.02	0.97 ± 0.02	5.20 ± 0.15
mixture of PDMS with hydrophilic silica					
first relaxation	153.2	0.195 ± 0.04	0.50 ● 0.05	0.80 ± 0.05	4.5 ● 0.4
	156.7	0.060 ± 0.01	0.50 ± 0.1	0.80 ± 0.05	5.1 ± 0.75
second relaxation	153.2	0.17 ± 0.03	0.45 ± 0.07	1.00 ± 0.05	1.8 ± 0.4
	156.7	0.23 ± 0.04	0.40 ± 0.05	1.00 ± 0.05	2.5 ± 0.4
	188.2	0.17 ± 0.03	0.40 ± 0.050	1.00 ± 0.05	5.6 ± 0.4
	199.3	0.15 ± 0.03	0.40 ± 0.05	1.00 ± 0.05	6.0 ± 0.5
	203.3	0.14 ± 0.03	0.40 ± 0.05	1.00 ± 0.05	6.3 ± 0.4
third relaxation	188.2	0.125 ± 0.02	0.40 ± 0.05	1.00 ± 0.05	1.5 ± 0.6
	199.3	0.16 ± 0.03	0.35 ± 0.06	1.00 ± 0.05	1.8 ± 0.5
	203.3	0.17 ± 0.03	0.33 ± 0.06	1.00 ± 0.05	2.0 ± 0.4

Table II
WLF Fit Parameters Obtained with a Fixed $f(T_0)$ of 1 Hz and Activation Enthalpies Determined by an Arrhenius Fit

	T_g/K	C_1	C_2/K	activation energy ΔH/(mol/kJ)
pure quenched PDMS				
first relaxation	147.2 ± 0.3	10.3 ± 1.3	13.5 ± 1.6	
second relaxation	154.6 ± 1.4	11.3 ± 1.0	32.9 ± 2.0	
pure annealed PDMS				67 ± 3
pure hydrophobic Aerosil				44 ± 5
pure hydrophilic Aerosil				43 ± 2
mixtures of PDMS with hydrophobic Aerosil				
first relaxation	143.1 ● 2	13.1 ± 2.8	18.7 ± 4.3	
second relaxation	153.9 ± 3.8	9.1 ± 2.5	20.6 ± 5.4	
third relaxation				53 ± 4
forth relaxation				104 ± 10
mixtures of PDMS with hydrophilic Aerosil				
first relaxation	144.8 ± 2	9.2 ± 2.5	13.2 ± 3.8	
second relaxation	146.9 ± 3.5	7.7 ± 2.9	26.5 ± 5	
third relaxation				32 ● 1.5

but with a similar activation energy of 43 ± 3 kJ/mol (Figure 3b), are observed. With increasing temperature the relaxation becomes narrower and higher but its strength $\Delta\epsilon$ decreases (see Table I).

For both types of Aerosil the relaxation can be explained by adsorbed water on the filler surface. The activation energies of water adsorption to silica gel of 31.5–42 kJ/mol have been determined by Lange.[27] These values are similar to the activation energies determined for the relaxation processes obtained for the hydrophilic and hydrophobic Aerosils of 43 and 44 kJ/mol, respectively. This water can give rise to a particle-bound conductivity resulting in a dielectric relaxation, the strength and frequency of which increase strongly with the conductivity of the particle. An Arrhenius-like temperature dependence of this conductivity can explain the evolution of this relaxation with temperature.[28,29] Thus the higher frequency of this process for hydrophilic Aerosil is explained by the larger amount of adsorbed water.

3.3. Mixtures of PDMS with Filler. 3.3.1. Hydrophilic Surface. For the quenched mixtures of PDMS with 50 vol % of hydrophilic Aerosil, the dielectric spectra (Figure 4a,b) showed three relaxations, which are enumerated in the following with rising temperatures (see Figures 4 and 5): As can be seen from the spectra at 153.2 and 156.7 K, respectively, in Figure 4a, the first relaxation of the most mobile fraction of dipoles, which has a half-width of about 3.1 decades, vanishes with increasing temperature, while at lower frequencies the second slightly broader relaxation increases in strength. In Figure 4b the spectra at higher temperatures (188.2 and 199.3 K) are shown. The high-frequency relaxation of this figure is identical with the second of the previous figure, while the loss peak at lower frequencies belongs to a third relaxation. The evolution of the processes with temperature is shown in the activation plot (Figure 5). Values of the three relaxation strengths $\Delta\epsilon$ are given in Table I. While the first two relaxation processes show a WLF-type temperature dependence, the third process shows an Arrhenius-type behavior with an activation energy of 32 kJ/mol.

In an activation plot the first relaxation of the mixture is located near the α-relaxation of the pure PDMS. The pure hydrophilic filler (Figure 3a) also has its relaxation in this frequency range, with a comparable dielectric strength $\Delta\epsilon$. However it shows a different activation behavior (compare Figure 3b and Figure 5) and, in contrast to the first relaxation in the mixture, it does not vanish with increasing temperature. This first relaxation in the filled system is therefore assigned to fluctuations of chains units, for which adsorption effects are negligible.

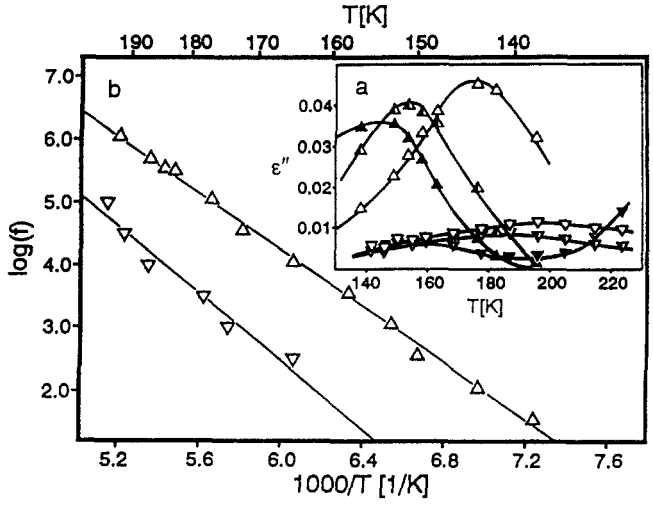

Figure 3. (a) Dielectric loss ϵ'' vs temperature and (b) activation plot for pure Aerosil. The symbols ▲, ▲, and △ denote data at frequencies of 110 Hz, 1.1 kHz, and 110 kHz for hydrophilic Aerosil, while ▼, ▼, and ▽ show the data points for hydrophobic filler at the same frequencies, respectively. (b) Maximum frequency f_{max} of the relaxation peak vs inverse temperature for pure fillers. The symbols △ and ▽ show data points for Aerosil with hydrophilic and hydrophobic surfaces, respectively. The solid lines are guides to the eye.

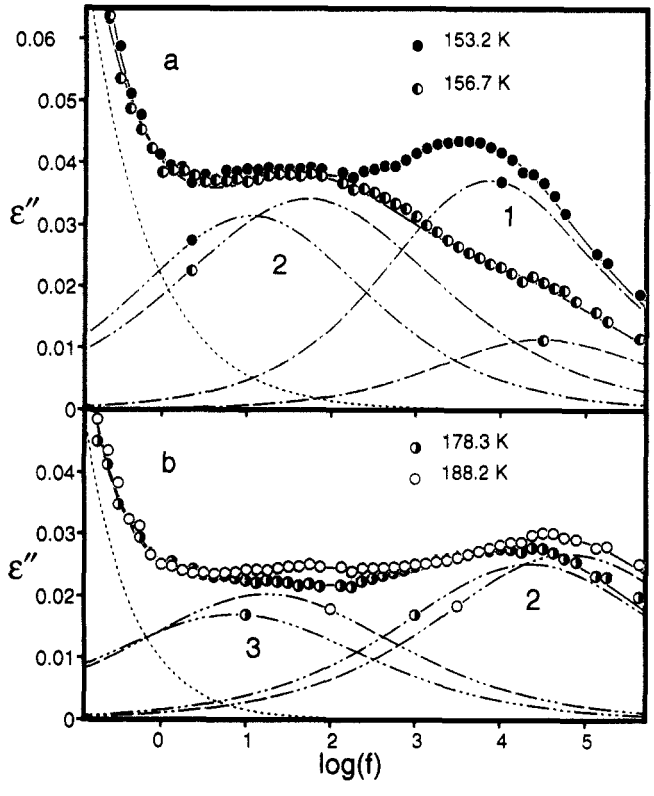

Figure 4. Dielectric loss ϵ'' vs frequency for a mixture of hydrophilic Aerosil with PDMS (50%/50%) at several temperatures. The solid lines are the fit curves, whereas the dashed lines describe the conductivity contribution to the fit (···) and the first/second/third relaxation processes (– · –/– ·· –/– ··· –). By symbols the curves of single relaxation processes are assigned to the corresponding temperatures.

The relaxation of the pure filler is uppressed or shifted in the mixture, but it may give contributions to the second or third relaxation in the mixtures. Since the crystallinity of the studied samples is negligible,[9,11] one can assume that the second and third relaxations of the mixture, which have no equivalent in the spectra of the single components, are assigned to relaxation processes in the adsorption layer,

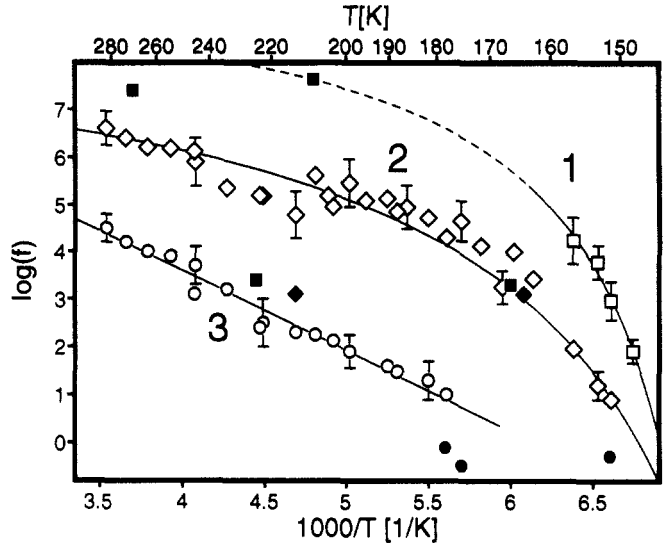

Figure 5. Transition map for the mixture of hydrophilic Aerosil with PDMS. The relaxation of directly adsorbed chain units is represented by the symbol ○, the interfacial relaxation by ◇, and the quasi-bulk relaxation by □. The data of the latter two processes are fitted by the WLF function. The temperature dependence of the slowest relaxation shows Arrhenius-like behavior. For comparison data from previous 1 H T_1 and T_2 experiments by NMR (■),[9] mechanical (●),[7] and dielectric spectroscopy (●)[6] are given. The last two measurements were carried out on filled PDMS networks.

i.e. relaxation processes taking place in the neighborhood of the Aerosil surface.

Well above T_g the relaxation processes within the adsorption layer (second and third) and outside of it (first) are well separated. This allows us to estimate the fraction of the adsorbed chain units from the relaxation strengths. At temperatures above 180 K the values of $\Delta\epsilon$ of the second and third relaxations sum up to a constant value of about 0.3 (Table I). Compared to the dielectric loss of the pure (noncrystalline) PDMS, 0.36 (taken into account the PDMS volume fraction of 50%), this indicates a joint volume fraction of 83% of the polymer for the adsorption layer, i.e. about 41% of the total volume.

From known values of the specific surface of the Aerosil, its volume fraction in the mixture and the fraction of the adsorption layer, the thickness of this layer was estimated for the following two alternative assumptions: (i) uniform covering of the filler particles by a PDMS layer of constant thickness; (ii) nonuniform covering due to a nearly dense packing of filler particles on a cubic lattice. These calculations led to values of 1 nm for the first and 2.5 nm for the second model in accordance with previous estimations.[9]

3.3.2. Hydrophobic Surface. From plots of the dielectric loss versus temperature for a quenched mixture of PDMS with 50 vol % of hydrophobic filler (Figure 6a,b), four relaxations can be separated. While the first relaxation (counted beginning at low temperatures for a given relaxation frequency) shows a narrow and high peak, the second and third ones are broader, lower, and overlapping in frequency. Therefore a quantitative analysis is not possible with high accuracy. The fourth relaxation is very weak and slow. The fit lines in Figure 6a represent functions according to eq 2.5.

WLF fits of the first and second relaxation (see activation plot in Figure 7) are better than Arrhenius fits (the corresponding fit parameters are listed in Table II), while the third and fourth relaxation show Arrhenius behavior. Their activation energies were determined to be 53 and 103 kJ/mol, respectively.

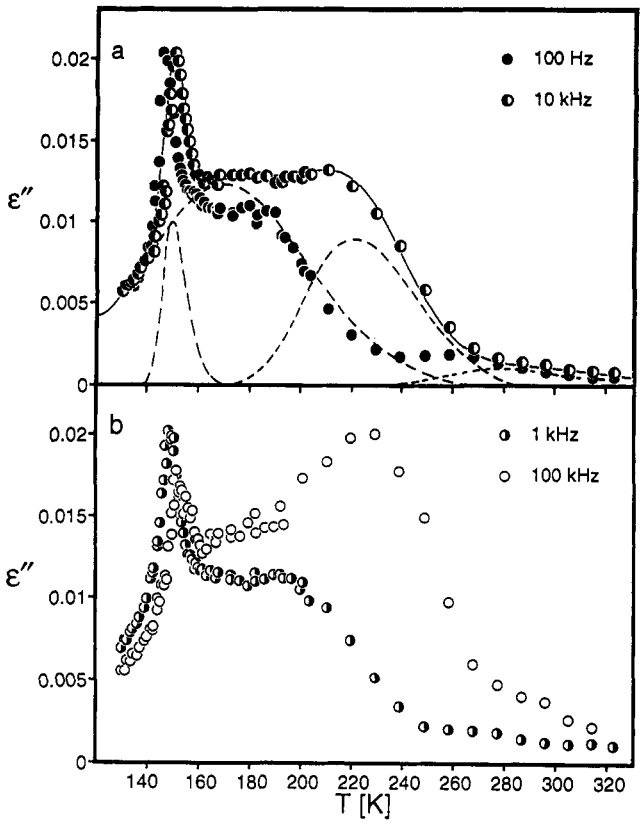

Figure 6. Dielectric loss ϵ'' versus temperature of a mixture of hydrophobic filler (A 380) with PDMS for several frequencies. In (a) the data are fitted by one multiple peak function (solid line), the components of which (four single peaks represented as dashed lines) are based on eq 2.5. For the sake of graphical clarity the fit lines are omitted in (b).

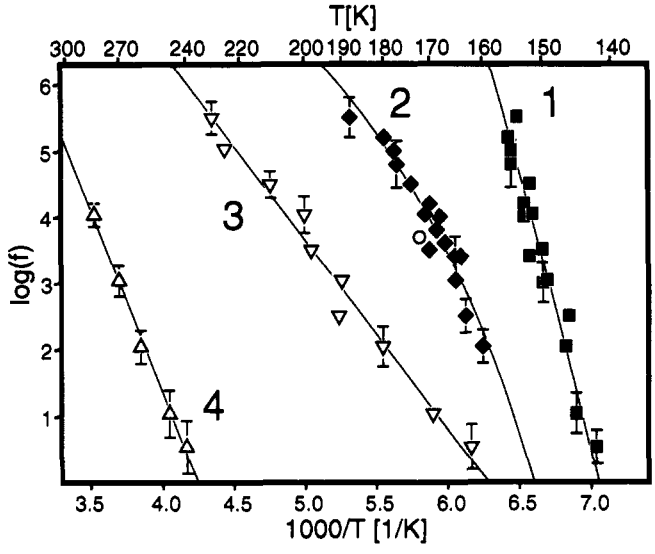

Figure 7. Transition map for a mixture of hydrophobic Aerosil with PDMS. Two of the four observed relaxations are assigned to chain units in the bulk region (■) and units with weak interaction to the filler (●), respectively. The assignment of the third (▽) and fourth relaxations (△) is not completely clear (see discussion in the text). By the symbol ○ a point from NMR experiments[9,30] for a relaxation in the adsorption layer is marked. The lines represent WLF (for 1 and 2) and Arrhenious fits (for 3 and 4).

A comparison of the first relaxation with the first of pure PDMS (compare Figure 7 with Figure 2) shows good agreement. Consequently, as in the case of PDMS mixtures with hydrophilic Aerosil, it can be assigned to chain units outside the adsorption layer.

The relaxation of the pure hydrophobic filler (see Figure 3) has roughly the same frequencies/temperatures in the activation plot as the second relaxation in the hydrophobic mixture. But, showing a pronounced WLF behavior, this second relaxation cannot be assigned to the filler. The relaxation of hydrophobic Aerosil shifts with the amount of adsorbed water on the Aerosil particles,[28,29] which is supposed to be smaller in the mixture than in the pure Aerosil because the covering PDMS reduces the access of air humidity. Thus, by a comparison of activation energies, the relaxation of the induced polarization of the pure filler can rather be assigned to the third relaxation process in the mixture. With this argumentation the second relaxation can be assigned to relaxation processes in the adsorption layer.

The molecular assignment of the third and fourth relaxation is not completely clear. Besides the relaxation of strongly adsorbed PDMS there are two possible reasons which may create or contribute to these processes, i.e. strongly adsorbed water at surface OH groups and reorientations of surface trimethylsilyl groups.

4. Conclusion

Molecular dynamics in PDMS–Aerosil mixtures and pure PDMS were studied by broad-band dielectric spectroscopy. Besides the α-relaxation of the amorphous phase, pure quenched PDMS, after cold crystallization, reveals the broader α_c-relaxation, which originates from chain motions in amorphous interstices between crystalline lamellae. The fractional volume of this restricted amorphous phase depends on the thermal history of the sample.

Mixtures of PDMS with hydrophilic Aerosil show two dielectric relaxation processes for chain units adjacent to the filler surface (adsorption layer) and one relaxation process for chain units outside of it. The thickness of the adsorption layer is estimated to be the range 1–2.5 nm.

The data for hydrophilic mixtures show reasonable agreement with previous dielectric and mechanical measurements[6,7] and with previous ^{1}H and ^{2}H NMR data (see Figure 5).[9,11,30] Mixtures of PDMS with hydrophobic Aerosil reveal four relaxations. Two of them were assigned to polymer chain units (in an adsorption layer and outside of it). Chain mobility in the adsorption layer for hydrophobic Aerosil is larger than for the hydrophilic one. The assignment of other relaxations is not obvious. They can result from the induced polarization of the Aerosil particles, from the reorientation of surface trimethylsilyl groups, and/or from strongly adsorbed and sterically hindered water molecules. The obtained data show good correlation with results from previous NMR experiments.[9,11,30]

Acknowledgment. The authors are indebted to Ulrich Maschke for providing the PDMS. V.M.L. would like to thank the Alexander von Humboldt Stiftung for a fellowship. The financial support by the Deutsche Forschungs Gemeinschaft in the framework of the Sonderforschungsbereich 262 is thankfully acknowledged.

References and Notes

(1) Litvinov, V. M.; Lavrukhin, B. D.; Zhdanov, A. A. *Polym. Sci. USSR* **1985**, *27*, 2789 and references therein.
(2) Semlyen, J. A.; et al. *Polymer* **1982**, *23*, 869.
(3) Törmälä, P. *J. Macromol. Sci. Rev. Macromol. Chem.* **1979**, *17*, 297.
(4) Adachi, H.; Adachi, K.; Ishida, Y.; Kotaka, T. *J. Polym. Sci., Polym. Phys. Ed.* **1979**, *17*, 851.
(5) Baird, M. E.; Sengupta, C. R. *Polymer* **1971**, *12*, 802.

(6) Martirosov, V. A.; Levin, V. Yu.; Zhdanov, A. A.; Slonimskii, G. L.; *Polym. Sci. USSR* **1988**, *30*, 1852.
(7) Yim, A.; Chahal, R. S.; St. Pierre, L. E. *J. Colloid Interface Sci.* **1973**, *43*, 583.
(8) Deryagin, B. V.; Karasev, V. V.; Lavygin, I. A.; Skorokhodov, I. I.; Khromova, E. N. *Dokl. Akad. Nauk SSSR* **1969**, *187*, 846.
(9) Litvinov, V. M. *Polym. Sci. USSR* **1988**, *30*, 2250 and references therein.
(10) Maschke, U.; Wagner, T.; Ballauff, M. Personal communication.
(11) Litvinov, V. M.; Spiess, H. W. *Makromol. Chem.* **1991**, *192*, 3005 and references therein.
(12) Kremer, F.; Boese, D.; Meier, G.; Fischer, E. W. *Prog. Colloid Polym. Sci.* **1980**, *80*, 129.
(13) Pugh, J.; Ryan, T. J. *IEEE Conf. Dielectric Materials, Measurements Applications* **1979**, *144*, 404.
(14) Havriliak, S.; Negami, S. *J. Polym. Sci., Part C* **1966**, *14*, 99.
(15) Havriliak, S.; Negami, S. *Polymer* **1967**, *8*, 161.
(16) Mott, N. F.; Davis, E. A. *Electronic Processes in non-crystalline Materials*; Clarendon Press: Oxford, UK, 1979.
(17) Williams, M. L.; Landel, R. F.; Ferry, J. D. *J. Am. Chem. Soc.* **1955**, *77*, 3701.
(18) Ferry, J. D. *Viscoelastic properties of polymers*; Wiley: Nw York, 1980.
(19) Doolittle, A. K. *J. Appl. Phys.* **1951**, *22*, 1471.
(20) Doolittle, A. K. *J. Appl. Phys.* **1952**, *23*, 236.
(21) Bloembergen, N.; Purcell, E. M.; Pound, R. V. *Phys. Rev.* **1948**, *73*, 679.
(22) Connor, T. M. *Trans. Faraday Soc.* **1964**, *60*, 1574.
(23) Böttcher, C. J. F.; Bordewijk, P. *Theory of electric polarization*; Elsevier: Amsterdam, **1978**; Vol. 2, 392.
(24) Semlyen, J. A.; et al. *Polymer* **1985**, *26*, 925.
(25) Andrianov, K. A.; Slonimskij, G. L.; Zhdanov, A. A.; Levin, Y.; Godovskij, Y. K.; Moskalenko, V. A. *J. Polym. Sci., Polym. Chem. Ed.* **1972**, *10*, 1.
(26) McCrum, N. G.; Read, B. E.; Williams, G. *Anelastic and Dielectric Effects in Polymer Solids*, Wiley, New York, 1967.
(27) Lange, K. R. *J. Colloid Sci.* **1965**, *20*, 231.
(28) Steeman, P. A. M.; Maurer, F. H. J. *Colloid Polym. Sci.* **1990**, *268*, 315.
(29) Steeman, P. A. M.; Maurer, F. H. J. *Polymer* **1991**, *32*, 523.
(30) Litvinov, V. M.; Zhdanov, A. A. *Polym. Sci. USSR* **1987**, *29*, 1133.